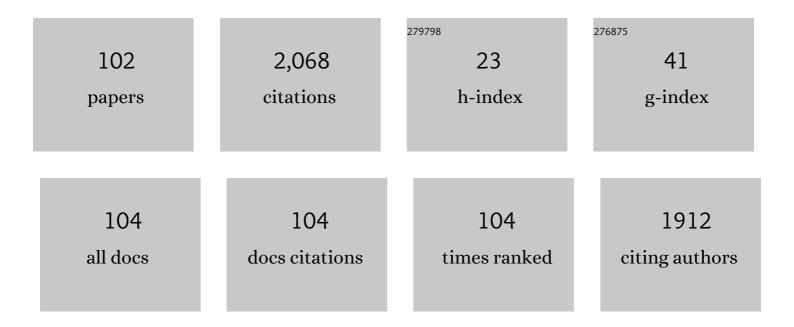
Leslie G Butler

List of Publications by Year in descending order

Source: https://exaly.com/author-pdf/7921949/publications.pdf Version: 2024-02-01



#	Article	IF	CITATIONS
1	Heavy Metal Stabilization in Municipal Solid Waste Combustion Dry Scrubber Residue Using Soluble Phosphate. Environmental Science & Technology, 1997, 31, 3330-3338.	10.0	162
2	Immobilization mechanisms in solidifiction/stabilization of cadmium and lead salts using portland cement fixing agents. Environmental Science & Technology, 1990, 24, 867-873.	10.0	129
3	29Si and 27Al MAS-NMR of NaOH-Activated Blast-Furnace Slag. Journal of the American Ceramic Society, 1994, 77, 2363-2368.	3.8	96

Translational symmetries in the linear-chain semiconductors K4[Pt2(P2O5H2)4X].cntdot.nH2O (X = Cl,) Tj ETQq0 0.0 rgBT /Overlock 10

5	Nuclear quadrupole coupling constants and hydrogen bonding. Molecular orbital study of oxygen-17 and deuterium field gradients in formaldehyde-water hydrogen bonding. Journal of the American Chemical Society, 1981, 103, 6541-6549.	13.7	78
6	Spectroscopic properties and redox chemistry of the phosphorescent excited state of octahydrotetrakis(phosphorus pentoxide)diplatinate(4-) ion (Pt2(P2O5)4H84-). Journal of the American Chemical Society, 1981, 103, 7796-7797.	13.7	77
7	Structural Characterization of MAO and Related Aluminum Complexes. 1. Solid-State27Al NMR with Comparison to EFG Tensors from ab Initio Molecular Orbital Calculations. Journal of the American Chemical Society, 2001, 123, 12009-12017.	13.7	69
8	Metal-metal interactions in binuclear platinum(II) diphosphite complexes. Resonance Raman spectra of the 1A1g(d.sigma.*)2 and 3A2u(d.sigma.*p.sigma.) electronic states of tetrakis(diphosphonato)diplatinate(4-) ion (Pt2(P2O5H2)44-). Journal of the American Chemical Society, 1983, 105, 5492-5494.	13.7	60
9	Immobilization of As, Cd, Cr and PB-containing soils by using cement or pozzolanic fixing agents. Journal of Hazardous Materials, 1990, 24, 145-155.	12.4	60
10	Methyaluminoxane (MAO) Polymerization Mechanism and Kinetic Model from Ab Initio Molecular Dynamics and Electronic Structure Calculations. Journal of the American Chemical Society, 2006, 128, 16816-16826.	13.7	51
11	Chemistry and spectroscopy of binuclear platinum diphosphite complexes. Inorganic Chemistry, 1985, 24, 4662-4665.	4.0	50
12	Single-Crystal 27Al NMR of Andalusite and Calculated Electric Field Gradients:  the First Complete NMR Assignment for a 5-Coordinate Aluminum Site. Journal of Physical Chemistry A, 1999, 103, 5246-5252.	2.5	48
13	Characterization and phosphate stabilization of dusts from the vitrification of MSW combustion residues. Waste Management, 1998, 18, 513-524.	7.4	46
14	Deuterium nuclear quadrupole resonance spectra of nonlinear hydrogen bonds. Journal of the American Chemical Society, 1982, 104, 1172-1177.	13.7	43
15	High-resolution neutron microtomography with noiseless neutron counting detector. Nuclear Instruments and Methods in Physics Research, Section A: Accelerators, Spectrometers, Detectors and Associated Equipment, 2011, 652, 400-403.	1.6	42
16	The structure of the cornified claw sheath in the domesticated cat (<i>Felis catus</i>): implications for the clawâ€shedding mechanism and the evolution of cornified digital end organs. Journal of Anatomy, 2009, 214, 620-643.	1.5	40
17	Petrographic and spectroscopic characterization of phosphate-stabilized mine tailings from Leadville, Colorado. Waste Management, 2002, 22, 117-135.	7.4	39
18	Neutron imaging of a commercial Li-ion battery during discharge: Application of monochromatic imaging and polychromatic dynamic tomography. Nuclear Instruments and Methods in Physics Research, Section A: Accelerators, Spectrometers, Detectors and Associated Equipment, 2011, 651, 320-328.	1.6	38

#	Article	lF	CITATIONS
19	Porosity detection in electron beam-melted Ti-6Al-4V using high-resolution neutron imaging and grating-based interferometry. Progress in Additive Manufacturing, 2017, 2, 125-132.	4.8	36
20	Structure of LiNO3: Point Charge Model and Sign of the 7Li Quadrupole Coupling Constant. Inorganic Chemistry, 1994, 33, 1363-1365.	4.0	32
21	Improved algorithm for processing grating-based phase contrast interferometry image sets. Review of Scientific Instruments, 2014, 85, 013704.	1.3	31
22	Protonâ€poor, gallium―and indium″oaded zeolite dehydrogenation catalysts. Catalysis Letters, 1998, 53, 111-118.	2.6	27
23	Oxygen-17 nuclear quadrupole double resonance. 6. Effects of hydrogen bonding. The Journal of Physical Chemistry, 1981, 85, 2738-2740.	2.9	26
24	NMR imaging of anisotropic solid-state chemical reactions using multiple-pulse line-narrowing techniques and proton T1 weighting. Journal of the American Chemical Society, 1992, 114, 125-135.	13.7	24
25	A broadband nuclear magnetic resonance spectrometer: Digital phase shifting and flexible pulse programmer. Review of Scientific Instruments, 1993, 64, 1235-1238.	1.3	24
26	Unusual asymmetry of methyl deuterium EFG in thymine: a solid state deuterium NMR and ab initio MO study. Journal of the American Chemical Society, 1987, 109, 2525-2526.	13.7	23
27	Three-Dimensional Chemical Analysis with Synchrotron Tomography at Multiple X-ray Energies:Â Brominated Aromatic Flame Retardant and Antimony Oxide in Polystyrene. Chemistry of Materials, 2004, 16, 4032-4042.	6.7	23
28	Olefin Rotation in the Solid State: A 13C, 1H, and 2H NMR Study of Rh(acac)(C2H4)2. Journal of the American Chemical Society, 1994, 116, 7445-7446.	13.7	21
29	INTERPRETATION OF ELECTRIC FIELD GRADIENTS AT DEUTERIUM AS MEASURED BY SOLID-STATE NMR SPECTROSCOPY. Journal of Coordination Chemistry, 1994, 32, 121-134.	2.2	21
30	Structural Characterization of Al10O6iBu16(μ-H)2, a High Aluminum Content Cluster: Further Studies of Methylaluminoxane (MAO) and Related Aluminum Complexes. Inorganic Chemistry, 2007, 46, 44-47.	4.0	21
31	Neutron interferometry detection of early crack formation caused by bending fatigue in additively manufactured SS316 dogbones. Materials and Design, 2018, 140, 420-430.	7.0	21
32	Observation of bridging and terminal metal hydrides by solid-state deuterium NMR spectroscopy: application to bis(cyclopentadienyl)zirconium dideuteride. Inorganic Chemistry, 1987, 26, 1381-1383.	4.0	20
33	Generation of binuclear (d8.d8)p.sigma. platinum and rhodium complexes by pulse radiolysis. Journal of the American Chemical Society, 1984, 106, 5143-5145.	13.7	19
34	High resolution three-dimensional visualization and characterization of coronary atherosclerosisin vitroby synchrotron radiation x-ray microtomography and highly localized x-ray diffraction. Physics in Medicine and Biology, 2002, 47, 4345-4356.	3.0	19
35	Deuterium quadrupole coupling constants and asymmetry parameters in metal hydrides: calculations of model systems representing three modes of metal-hydrogen bonding. Inorganic Chemistry, 1987, 26, 3001-3004.	4.0	18
36	Rotation of the cyclopentadienyl ligand in bis(.mucarbonyl)bis(carbonylcyclopentadienyliron)(Fe-Fe) in the solid state as determined from solid-state deuterium NMR spectroscopy. Inorganic Chemistry, 1990, 29, 741-747.	4.0	18

#	Article	IF	CITATIONS
37	Solid-state deuterium NMR spectroscopy of d5-phenol in white portland cement: a new method for assessing solidification/stabilization. Environmental Science & amp; Technology, 1993, 27, 1426-1433.	10.0	17
38	Deuterium quadrupole coupling constants and asymmetry parameters in bridging metal hydride complexes. Journal of the American Chemical Society, 1991, 113, 9090-9096.	13.7	16
39	Pulsed 81Br Nuclear Quadrupole Resonance Spectroscopy of Brominated Flame Retardants and Associated Polymer Blends. Chemistry of Materials, 1998, 10, 1291-1300.	6.7	16
40	27Al field-swept and frequency-stepped NMR for sites with large quadrupole coupling constants. Solid State Nuclear Magnetic Resonance, 2000, 16, 63-67.	2.3	16
41	Karplus-type relationship for quadrupole coupling constants and asymmetry parameters for substituted acetic acids. Journal of the American Chemical Society, 1988, 110, 343-347.	13.7	15
42	Bond Breaking in the Chemical Vapor Deposition Precursor (1,1,1,5,5,5-Hexafluoro-2,4-pentanedionato)(.eta.2-1,5-cyclooctadiene)copper(I) Studied by Variable-Temperature X-ray Crystallography and Solid-State NMR Spectroscopy. Chemistry of Materials, 1994, 6, 587-595.	6.7	15
43	Solid-State2H MAS NMR Studies of TNT Absorption in Soil and Clays. Environmental Science & Technology, 2001, 35, 2973-2978.	10.0	15
44	The 10B and 11B nuclear quadrupole resonance spectra of boric acid. Journal of Magnetic Resonance, 1981, 42, 120-131.	0.5	14
45	15 T, 4.2 K field-swept 27Al NMR spectroscopy. Chemical Physics Letters, 1994, 221, 65-67.	2.6	14
46	Synchrotron X-ray Microtomography, Electron Probe Microanalysis, and NMR of Toluene Waste in Cement. Environmental Science & amp; Technology, 2000, 34, 3269-3275.	10.0	13
47	Synchrotron X-ray microtomography, X-ray absorption near edge structure, extended X-ray absorption fine structure, and voxel imaging of a cobalt–zeolite-Y complex. Materials Research Bulletin, 2001, 36, 1595-1602.	5.2	12
48	Carbon-13 NMR chemical shielding tensor of the bridging methylene unit in cis-(.muCH2)(.muCO)[FeCp(CO)]2. Journal of the American Chemical Society, 1991, 113, 4831-4838.	13.7	11
49	Nonlinear least-squares fitting procedure for solid-state NMR powder patterns. Concepts in Magnetic Resonance, 1992, 4, 205-226.	1.3	11
50	High-field 19.6T 27Al solid-state MAS NMR of in vitro aluminated brain tissue. Journal of Magnetic Resonance, 2004, 170, 257-262.	2.1	11
51	Determination of the charge on carbon in a bridging methylene iron dimer with solid-state deuterium NMR spectroscopy. Journal of the American Chemical Society, 1987, 109, 5529-5531.	13.7	10
52	Solid-state carbon-13 NMR chemical shift tensors in square-planar tetracyanometalates (M = nickel,) Tj ETQq0 0	0 rgBT /Ov	verlock 10 Ti
53	Tools and strategies for processing diffusion-ordered 2D NMR spectroscopy (DOSY) of a broad, featureless resonance: an application to methylaluminoxane (MAO). Analytical and Bioanalytical Chemistry, 2004, 378, 1574-1578.	3.7	10

⁵⁴Neutron Radiography, Tomography, and Diffraction of Commercial Lithium-ion Polymer Batteries.1.21054Physics Procedia, 2013, 43, 331-336.

#	Article	IF	CITATIONS
55	Neutron Imaging of Laser Melted SS316 Test Objects with Spatially Resolved Small Angle Neutron Scattering. Journal of Imaging, 2017, 3, 58.	3.0	10
56	Strengthening spatial reasoning: elucidating the attentional and neural mechanisms associated with mental rotation skill development. Cognitive Research: Principles and Implications, 2020, 5, 20.	2.0	10
57	Transient spectroscopy of the lowest excited states of binuclear rhodium(I) isocyanides. The Journal of Physical Chemistry, 1986, 90, 5567-5570.	2.9	9
58	Structures of three related biphenyl compounds: 4,4'-biphenyldiol, 3,3',5,5'-tetra-tert-butyl-4,4'-biphenyldiol, and 3,3',5,5'-tetra-tert-butyl-1,1'-bicyclohexa-2,5-dienylidene-4,4'-dione. Acta Crystallographica Section C: Crystal Structure Communications, 1990, 46, 919-922.	0.4	9
59	Multiple pulse NMR imaging of polymers and chemistry. Magnetic Resonance Imaging, 1992, 10, 789-791.	1.8	9
60	11B imaging with field-cycling NMR as a line narrowing technique. Chemical Physics Letters, 1993, 206, 464-466.	2.6	9
61	Field-Cycling 14N NQR Imaging with Spatial and Frequency Resolution. Journal of Magnetic Resonance Series A, 1995, 112, 92-95.	1.6	9
62	Automated, Web-Based, Second-Chance Homework. Journal of Chemical Education, 2001, 78, 1704.	2.3	9
63	A microtomography beamline at the Louisiana State University Center for Advanced Microstructures and Devices synchrotron. Review of Scientific Instruments, 2002, 73, 1521-1523.	1.3	8
64	Algorithms for three-dimensional chemical analysis via multi-energy synchrotron X-ray tomography. Nuclear Instruments & Methods in Physics Research B, 2007, 262, 117-127.	1.4	8
65	Analysis of Flame Retardancy in Polymer Blends by Synchrotron X-ray K-edge Tomography and Interferometric Phase Contrast Movies. Journal of Physical Chemistry B, 2016, 120, 2612-2624.	2.6	8
66	Early detection of fracture failure in SLM AM tension testing with Talbot-Lau neutron interferometry. Additive Manufacturing, 2018, 22, 658-664.	3.0	8
67	Structure of 4-nitrobenzaldehyde. Acta Crystallographica Section C: Crystal Structure Communications, 1989, 45, 2016-2018.	0.4	7
68	Synchrotron X-ray Tomography for 3D Chemical Distribution Measurement of a Flame Retardant and Synergist in a Fiberglass-Reinforced Polymer Blend. Journal of Physical Chemistry B, 2010, 114, 2-9.	2.6	7
69	Synchrotron X-ray tomography for 3D chemical diffusion measurement of a flame retardant in polystyrene. Nuclear Instruments and Methods in Physics Research, Section A: Accelerators, Spectrometers, Detectors and Associated Equipment, 2007, 582, 202-204.	1.6	6
70	Ab Initio Calculation of 81Br Nuclear Quadrupole Resonance Transition Frequencies for Brominated Aromatics (Flame Retardants). Journal of Physical Chemistry A, 1999, 103, 8088-8092.	2.5	5
71	Development of grating-based x-ray Talbot interferometry at the advanced photon source. AIP Conference Proceedings, 2012, , .	0.4	5
72	Edge Enhancement in Cold Neutron Imaging: A Comparison of Experiments at Edges and Interfaces with Ray-tracing based on Refraction and Reflection. Physics Procedia, 2013, 43, 149-160.	1.2	5

#	Article	IF	CITATIONS
73	Highâ€power radio frequency irradiation system with automatic tuning. Review of Scientific Instruments, 1982, 53, 984-988.	1.3	4
74	Structure of a new polymorph of cis-[(μ-CH2)(μ-CO){Fe(η5-C5H5)CO}2]. Acta Crystallographica Section C: Crystal Structure Communications, 1992, 48, 644-650.	0.4	4
75	Low-temperature (4.2 K) 23Na and 27Al swept-field nuclear magnetic resonance spectroscopy of zeolites: observation of framework and non-framework aluminum sites. Microporous Materials, 1995, 4, 265-271.	1.6	4
76	Zeeman-effect studies of the electronic absorption spectrum of octachlorodirhenate(2â^') (Reî—½Re) in pulsed 50-Tesla magnetic fields. Inorganica Chimica Acta, 1996, 243, 309-316.	2.4	4
77	Burning Issues in Tomography Analysis. Computing in Science and Engineering, 2008, 10, 78-81.	1.2	4
78	Boron-10 and boron-11 nuclear quadrupole resonance spectrum of decaborane[14]. Journal of Magnetic Resonance, 1985, 65, 472-480.	0.5	3
79	A karplus-type relationship for deuterium quadrupole coupling constants. II. Inequivalent Cî—,2H sites in substituted acetic acids. Journal of Magnetic Resonance, 1989, 82, 76-85.	0.5	3
80	The Faraday effect in Cd0.57Mn0.43Te in high magnetic field. Physica B: Condensed Matter, 1998, 246-247, 319-322.	2.7	3
81	Imaging tissue structures: assessment of absorption and phase-contrast x-ray tomography imaging at 2ndand 3rdgeneration synchrotrons. , 2006, 6318, 629.		3
82	Real-time observation of hydrogen absorption by LaNi5 with quasi-dynamic neutron tomography. Nuclear Instruments & Methods in Physics Research B, 2014, 324, 95-101.	1.4	3
83	Wavepy - python package for x-ray grating interferometry with applications in imaging and wavefront characterization. AIP Conference Proceedings, 2019, , .	0.4	3
84	Intact, Commercial Lithium-Polymer Batteries: Spatially Resolved Grating-Based Interferometry Imaging, Bragg Edge Imaging, and Neutron Diffraction. Applied Sciences (Switzerland), 2022, 12, 1281.	2.5	3
85	Learning the Student Names in Large Classes: An Application of Multimedia Technology. Journal of Chemical Education, 1995, 72, 610.	2.3	2
86	Chemical systems for exploration of high magnetic field effects. International Journal of Quantum Chemistry, 1997, 64, 607-611.	2.0	2
87	Study of Morphological Changes in MgH2 Destabilized LiBH4 Systems Using Computed X-ray Microtomography. Materials, 2012, 5, 1740-1751.	2.9	2
88	Non-destructive evaluation of additively manufactured polymer objects using X-ray interferometry. Additive Manufacturing, 2018, 24, 364-372.	3.0	2
89	14N nuclear quadrupole resonance study of the nucleotide base pair 1-methylcytosine hemihydroiodide hemihydrate. Journal of Magnetic Resonance, 1981, 44, 483-487.	0.5	1
90	Displaying the results from NMR pulse sequence simulations as stereo diagrams. Journal of Magnetic Resonance, 1991, 91, 396-399.	0.5	1

#	Article	IF	CITATIONS
91	Data translation from instrument specific to ASCII. Computers & Chemistry, 1992, 16, 71-72.	1.2	1
92	Resolving two inequivalent sites with deuterium MAS NMR. Journal of Magnetic Resonance, 1992, 99, 292-300.	0.5	1
93	Some aspects of data processing for an optical absorption experiment in a pulsed 1000-Tesla magnet. International Journal of Quantum Chemistry, 1998, 70, 797-804.	2.0	1
94	<title>Synchrotron x-ray microtomography and solid state NMR of environmental wastes in cement</title> . , 1999, , .		1
95	The 3D chemical distribution of a flame retardant in a fiberglass-reinforced polymer blend as measured with synchrotron x-ray tomography. , 2006, , .		1
96	Recent applications of X-ray grating interferometry imaging to evaluate flame retardancy performance of brominated flame retardant. Polymer Degradation and Stability, 2017, 138, 1-11.	5.8	1
97	Structure of the tetrahedral cobalt cluster [Co4(η5-C5H5)2(CO)7]. Acta Crystallographica Section C: Crystal Structure Communications, 1987, 43, 2283-2285.	0.4	0
98	Quantum jumps in magneto-optical effects and magnetization of rare-earth compounds in ultrahigh magnetic fields. Physica B: Condensed Matter, 1998, 246-247, 315-318.	2.7	0
99	Tomography at the Louisiana State University CAMD synchrotron: applications to polymer blends. , 2002, 4503, 54.		0
100	Algorithms for three-dimensional chemical analysis with multi-energy tomographic data. , 2004, , .		0
101	A New Tomography Beamline at a Wiggler Port at the Center for Advanced Microstructures and Devices (CAMD) Storage Ring. AIP Conference Proceedings, 2007, , .	0.4	0
102	Improving the workflow of tomography studies for the polymer additives industry. , 2012, , .		0